

Optical Heterodyne Detected Transient Grating for the Separations of Phase and Amplitude Gratings and of Different Chemical Species

Masahide Terazima*

Department of Chemistry, Graduate School of Science, Kyoto University, Kyoto, 606-8502, Japan

Received: February 24, 1999; In Final Form: July 15, 1999

The sensitivity and stability of an optical heterodyne detected transient grating (OHD-TG) method without an active phase control system was examined, and the system was used to separate the phase and amplitude gratings. From the absorptive component at 633 nm after the photoexcitation of a photochromic molecule (a spiropyran molecule), the diffusion constant of only the merocyanine form is selectively determined. The phase grating component consists of both the spiro and merocyanine contributions. However, since the contribution of the merocyanine form is still predominant over the spiro form in the phase grating signal, the diffusion process of the spiro form cannot be observed clearly. By adjusting the phase between the local oscillator and probe fields, the contribution of the merocyanine form can be selectively reduced and the diffusion constant of the spiro form is successfully measured. The result shows that the selective reduction of one species by the OHD-TG technique has a great advantage for studying photochemical reactions.

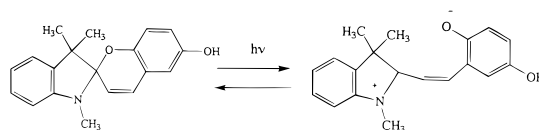
1. Introduction

For studies on photophysical and photochemical processes, the transient grating (TG) technique has proven to be a very powerful method and many applications have been reported.^{1–8} The usefulness comes from the flexibility of this method such as wavelengths and the polarizations for the excitation and probe lights as well as a high time resolution and a high sensitivity. This technique can detect a variety of phenomena; optical Kerr effect of the electronic and the nuclear responses (orientational dynamics), thermal energy from the nonradiative transition or from the chemical enthalpy change, creation (depletion) of the excited states (ground state), and creation of new chemical species. These dynamics appear as the TG signal through the refractive index changes (phase grating) and the absorption changes (amplitude grating). For a correct interpretation, these different origins should be discriminated. The wavelength dependence, polarization selection, characteristic time scale, temporal profile, absolute signal intensity, etc. have been used as criteria of the discrimination. However, the complete distinction is still a rather difficult task. One of the most serious tangles occurs between the phase and amplitude gratings in the signal. The homodyne detected TG signal under the weak diffraction limit may be given by¹

$$I_{\text{TG}} = \alpha(\delta n(t))^2 + \beta(\delta k(t))^2 \quad (1)$$

where α and β are constants and δn and δk are the change of the refractive index and absorbance, respectively. If the grating is composed solely of the phase or amplitude grating, the material response can be obtained by simply taking the square root of the signal. However, if these contributions exist simultaneously in the signal, the material response cannot be obtained unless the exact amplitudes of these components are known. The observed temporal profile could be completely different from the real response because of such an interference effect.

SCHEME 1



One of the approaches to achieve the distinction between the phase and amplitude gratings is the optical heterodyne detection (OHD) technique, which utilizes the interference between the signal field and a local oscillator (LO) field. Owing to various advantages, including the merit of the separation, the OHD method in the TG technique was implemented with either active or passive stabilization methods so far.^{9–16} Each method has advantages and some limitations. Recently we constructed a OHD-TG setup without an active phase feedback system by a slight modification of a conventional TG system using a pulsed laser for the excitation and a cw laser for the probing.¹⁹ This system is as flexible as a conventional TG setup and stable enough even in an ordinary laboratory without a precise temperature control. We have demonstrated that the linearized TG signal by the OHD-TG method can reveal a weak feature, which is easily missed by the homodyne detection.¹⁹ Recently, a heterodyne detected four wave mixing experiment with a similar strategy was reported.²⁰

Despite many advantages and several demonstrations of the OHD-TG technique to date, studies of the separation of the phase and amplitude grating components just recently began.^{17,18} In this article, we report the OHD-TG method for the separation of the phase and amplitude grating contributions. The OHD system was applied to a photochromic reaction of 1',3',3'-trimethyl-6-hydroxyspiro(2H-1-benzopyran-2,2'-indoline) (THS) (Scheme 1).

This is one of the spiropyran, which are well known as photochromic molecules, and the physical properties of these spiropyran are of great interest.^{21,22} On UV photoirradiation of the spiro forms, they are converted to colored merocyanine forms. The time-resolved TG method was used to study the

* E-mail: mterazima@kuchem.kyoto-u.ac.jp.

molecular dynamics of a spiro-merocyanine previously.²² However, for THS, a strong absorption band of the merocyanine form is located at the wavelength of the He–Ne laser (633 nm), which is frequently used for the probe light. Under this probing, the TG signal is dominated by the absorptive contribution and most of the signal comes from the merocyanine form. Hence, any molecular information of the spiro form is hardly obtained by this TG system. In this paper, the absorptive and refractive contributions from THS are separated by the OHD-TG system. Not only that, we can selectively reduce a contribution of the merocyanine form by using a merit of the phase adjustment between the probe and LO lights. Using this selective reduction, the diffusion constants of the merocyanine and the spiro form are simultaneously determined.

2. Experimental Section

A block diagram of the experimental setup for the OHD-TG system was reported previously.¹⁹ The third harmonics of a Nd:YAG laser (Spectra Physics, GCR170) was used for the excitation light (pulse width ~ 10 ns). A typical excitation laser power was $0.5\sim 1 \mu\text{J}/\text{pulse}$ for the OHD-TG detection. The beam was split into two with nearly equal intensities by a beam splitter and crossed at a sample by a lens to create the transient grating. The grating wavenumber can be freely adjustable in a range of $0.5\sim 4 \times 10^6 \text{ m}^{-1}$. The excitation beams were not tightly focused on the sample to avoid any multiphoton process or higher order reaction (spot size $\sim 1 \text{ mm}\phi$). Also, the moderate spot size is important to reduce the thermal lens contribution (vide infra). A He–Ne laser beam was split by a glass plate into two beams with a 1:10 intensity ratio. The stronger beam was introduced to the crossing region of the excitation beams at an angle that satisfies the Bragg condition. The interaction of these three beams creates the TG signal. The weaker beam from the He–Ne laser was further attenuated (a factor of 10^3) by a neutral density (ND) filter. The filter was slightly tilted and used for a fine adjustment of the phase of the LO field to the probe field by changing the optical path length inside the filter. Since this optical length change during the angle adjustment is less than the wavelength of the LO light, the LO light intensity change by the angle change is negligible. The angle of the ND filter was adjusted by monitoring the signal to obtain an appropriate phase difference (vide infra). The signal and LO light were overlapped on a pinhole (diameter ~ 5 mm) and the signal was detected by a photomultiplier (Hamamatsu R928). The system was constructed compactly and placed on a solid plate. Sometimes the system was covered with a box to prevent air current. There is, however, still room for inserting polarizers and waveplates to control the polarizations of the excitation probe and LO beams. The signal was averaged by a digital oscilloscope (Tektronix 2430A) and a microcomputer. The repetition rate of the excitation was $3\sim 4$ Hz. The TG experiment was performed at a laboratory without a precise temperature control system.

THS (Acros Organics), nitrobenzene (Wako Chem. Co.), and ethanol (spectrograde from Nakalai Tesque) were used as received. The concentration of THS was 1.0 mM. The sample solution was stirred between each measurement to avoid the accumulation of the merocyanine form. The accumulation during the measurement (8 shots) was found to be negligible under this weak laser power and slow repetition rate condition.

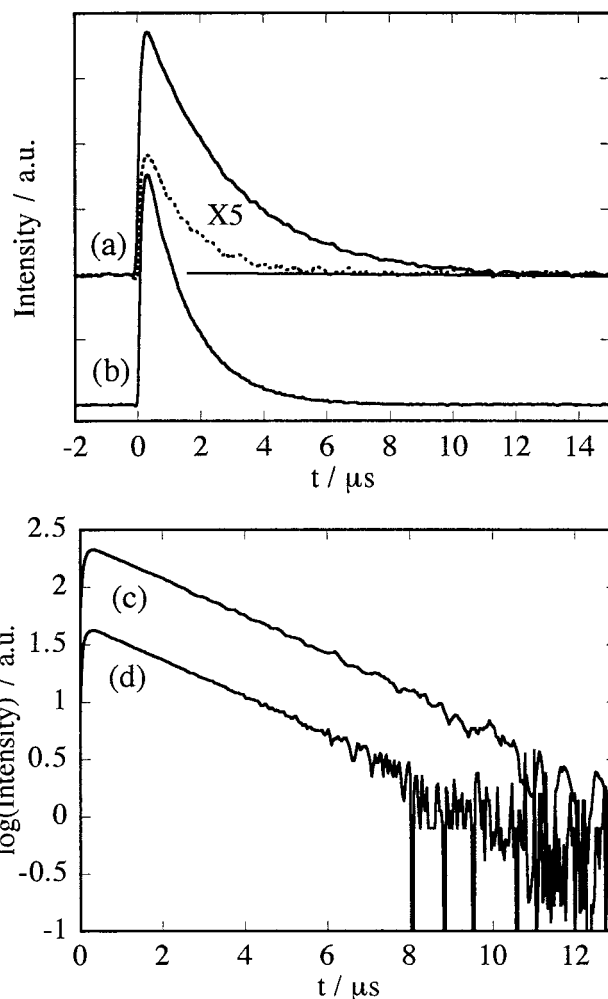


Figure 1. (a) Homodyne detected TG signal (dotted line, amplified by a factor of 5) and OHD-TG signal (solid line) after photoexcitation of nitrobenzene in benzene. (b) Homodyne detected TG signal with a higher excitation laser power. (c) OHD-TG signal in a semilogarithmic scale. (d) A semilogarithmic plot of the square root of the homodyne detected TG signal of (b). The intensity of the homodyne signal is shifted downward to avoid the overlap.

3. Results and Discussion

3-1. Stability and Sensitivity. Figure 1(a) shows the homodyne detected TG signal after the photoexcitation of nitrobenzene in benzene. Since the lifetimes of the excited states of nitrobenzene are much shorter than the response time of our system,²³ the signal consists of only the thermal grating component that comes from the thermal energy by the non-radiative relaxation. Since the thermal grating is almost a pure phase grating, the homodyne detected signal in this case is given by

$$I_{\text{TG}}(t) = \alpha(\delta n_{\text{th}}(t))^2 \quad (2)$$

$$\delta n_{\text{th}}(t) = \delta n_{\text{th}}^0 \exp(-D_{\text{th}}q^2t)$$

where δn_{th}^0 is the initial refractive index change of the thermal grating, D_{th} is the thermal diffusivity, and q is the grating wavenumber.

When the LO light is introduced to the grating region and overlapped on the detector, the signal is significantly enhanced. The detected light intensity under this heterodyne condition (I_{tot})

may be given by¹

$$I_{\text{tot}}(t) = A|E_{\text{LO}} + E_{\text{S}}(t)|^2 \quad (3)$$

$$= A\{|E_{\text{LO}}|^2 + (E_{\text{LO}}^*E_{\text{S}}(t) + E_{\text{LO}}E_{\text{S}}(t)^*) + |E_{\text{S}}(t)|^2\}$$

where A is a constant and E_{LO} and $E_{\text{S}}(t)$ are the electric fields of the LO and signal lights, respectively. $|E_{\text{LO}}|^2$ gives a constant background of $I_{\text{LO}} = A|E_{\text{LO}}|^2$. If we express the signal field as $E_{\text{S}}(t) = \chi^{(3)}(t)E_{\text{p}}I_{\text{ex}}$ (E_{p} , electric field of the probe light, I_{ex} , the intensities of the excitation light, and $\chi^{(3)}(t)$, material response) and $E_{\text{LO}} = ae^{i\Delta\phi}E_{\text{p}}$ (a ; real), I_{tot} is given by

$$I_{\text{tot}}(t) = I_{\text{LO}} + \{2a\chi^{(3)'}(t)\cos\Delta\phi + 2a\chi^{(3)''}(t)\sin\Delta\phi + |\chi^{(3)}(t)|^2I_{\text{ex}}\}I_{\text{ex}}I_{\text{p}} \quad (4)$$

where $\chi^{(3)'}$ (t) and $\chi^{(3)''}$ (t) are, respectively, the real and imaginary parts of the material response, $\Delta\phi$ is the phase difference between the LO and probe lights, and I_{p} is the intensity of the probe light. Here we assume that our system response time is fast enough compared with the material response time. If the signal field is negligibly weak compared with E_{LO} , ($|E_{\text{LO}}| \gg |E_{\text{S}}|$), or the homodyne contribution is subtracted from the signal, the observed OHD-TG signal intensity (I_{OHD}) is given by

$$I_{\text{OHD}}(t) = 2a\{\chi^{(3)'}(t)\cos\Delta\phi + \chi^{(3)''}(t)\sin\Delta\phi\}I_{\text{ex}}I_{\text{p}} \quad (5)$$

For the signal from nitrobenzene, $\chi^{(3)'}$ (t) is $\delta n_{\text{th}}(t)$ and $\chi^{(3)''}$ (t) = 0. Throughout this study, we measured the TG signals with the LO light (I_{tot}) and without the LO light (homodyne signal) under the same condition and subtracted the weak homodyne signal from I_{tot} to obtain the OHD-TG signal.

In addition to the enhancement of the signal intensity, the decay rate of the OHD-TG signal is 2 times smaller than that of the homodyne signal, which indicates that the signal is now linearized with respect to the material response.

When we compare the OHD-TG signal with the homodyne detected signal under the same excitation power, the high sensitivity of the OHD-TG signal is apparent (Figure 1(a)). If we can increase the excitation power, the signal-to-noise ratio (S/N) of the homodyne detected signal can be much improved, because one of the advantages of homodyne detection is the background-free character. For the purpose of comparison, the excitation laser power is increased so that the homodyne detected signal intensity becomes about equal to that of the OHD-TG signal (Figure 1(b)). The high S/N during the initial part of the homodyne detected signal (0~4 μs) compared with the OHD-TG signal is apparent. However, since the decay rate of the homodyne detected signal is a factor of 2 larger than the actual rate constant, the signal decays quickly. As a consequence, the quality of the OHD-TG signal against the homodyne detected signal in a longer time scale (e.g., after 6 μs) is better (Figure 1(c) and (d)). Previously, the advantage of the linearization of the signal was clearly shown by revealing a weak feature of the species grating signal of Methyl red.¹⁹ Furthermore, for quantitative studies of photochemical reactions, it is frequently demanded that the excitation power should be as weak as possible to avoid a saturation effect or higher order reactions. In such a case, the advantage of OHD-TG is clear.

One of the difficulties of the OHD-TG method is to achieve phase stability. Since our system is a real time detection system, it takes only 30 μs for one recording. Even for an average of eight times, it takes only 2 s at the 4 Hz repetition rate. There

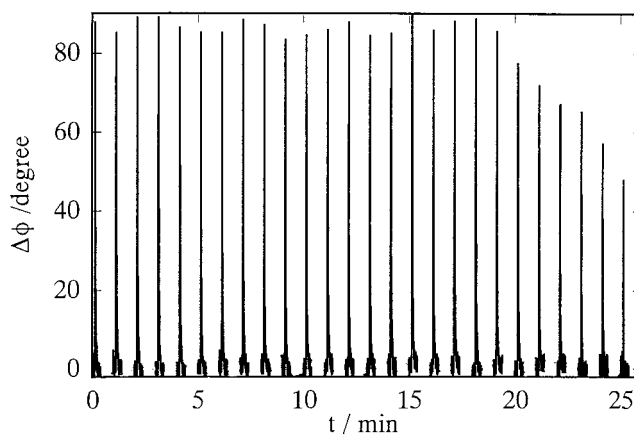


Figure 2. Stability of the phase between the LO and probe ($\Delta\phi$). The signal is the thermal grating from nitrobenzene in benzene.

was almost no phase fluctuation ($|\Delta\phi| \leq 2^\circ$) during that period. For monitoring long-term stability, the signal was averaged eight times (during 2 s) at 1 min intervals and is shown in Figure 2. Since the signal is the almost pure phase grating, the maximum intensity of the peak corresponds to $\Delta\phi = 0^\circ$ and the intensity decreases with deviating the phase difference from $\Delta\phi = 0^\circ$. The signal disappears at $\Delta\phi = 90^\circ$, and 270° . Hence, the peak intensity directly reflects the phase fluctuation. (Since the signal lasts only 10 μs and the signal during that short period cannot be seen in the time scale of Figure 2, the time range of the signal in the figure was expanded for clear viewing. The intensity fluctuation by a laser power fluctuation was corrected.) In this case, the phase was stable during ~15 min within $|\Delta\phi| \leq 5^\circ$ and then gradually shifted. In many cases, we observed that the phase stayed within $|\Delta\phi| \leq 5^\circ$ during 10~20 min. There may be several origins for the phase shift under this condition, such as air currents, temperature drift, and laser beam pointing fluctuation. We do not determine which factor most seriously affects the phase fluctuation and the drift. We may speculate, however, that the air currents and the temperature drift are the main origins because the drift becomes much smaller when we cover the system with a box. If the temperature is well regulated, the phase stability may be much better. However, even under present conditions, the phase stability is good enough for a series of many measurements. The phase difference can be arbitrarily adjusted by tilting the ND filter during that period. Even if time dependent phase shift occurs, the phase moves slowly to one direction most of the time. Sometimes, this automatic phase shift could be used for measuring the OHD-TG signal at different phase angles.

3-2. OHD-TG Signals of THS. Figure 3(a) shows the homodyne detected TG signal after the photoexcitation of THS in ethanol (LO light is blocked). The signal consists of two contributions; the thermal grating and the species grating signals. The latter is due to the photochromic reaction of THS.²² The refractive index change (δn_{sp}) and absorption change (δk_{sp}) due to this reaction may be expressed by²²

$$\delta n_{\text{sp}}(t) = \delta n_1^0 \exp(-D_s q^2 t) + \delta n_2^0 \exp(-D_m q^2 t) \quad (6)$$

$$\delta k_{\text{sp}}(t) = \delta k_2^0 \exp(-D_m q^2 t)$$

where δn_1^0 , δn_2^0 , and δk_2^0 are preexponential factors and D_s and D_m are the diffusion constant of the spiro and merocyanine forms, respectively. Here we neglected the contribution of the spiro form in the amplitude grating, because of no absorption band at 633 nm. Furthermore, we also neglected the back

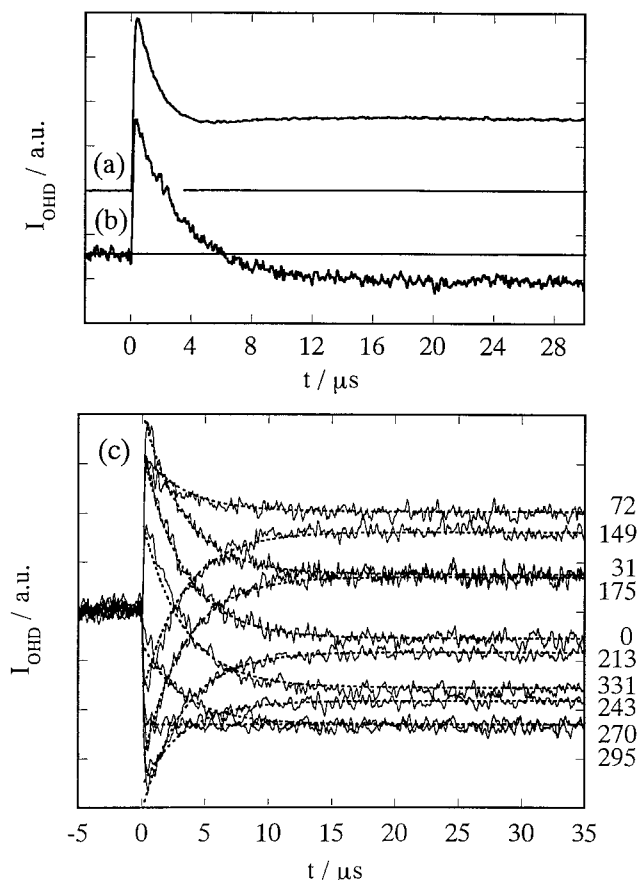


Figure 3. (a) Homodyne detected TG and (b) OHD-TG signals ($\Delta\phi = 0$) after the photoexcitation of THS in ethanol. The excitation laser power of (b) is about 1/4 of (a). The numbers listed in the figure (c) indicate the phase angles between the probe and LO fields. They were determined by the signal fitting with eq 5. The calculated curve is shown by the dotted line. The error of the phase angle is $\pm 2^\circ$.

reaction from the merocyanine to spiro form, because the back reaction is much slower than this recording range. As a consequence of the quadratic nature of the homodyne detected signal (eq 1), the temporal profile is not a simple exponential decay, but the interference between δn_{th} and δn_{sp} is apparent as a dip between the thermal grating and the species grating signals. The appearance of the interference dip indicates that the signs of δn_{th}^0 and $\delta n_1^0 + \delta n_2^0$ are opposite. Since, in many solvents, δn_{th}^0 is generally negative, $\delta n_1^0 + \delta n_2^0$ should be positive. The apparent decay rate constant of the thermal grating in this case should not be $2D_{th}q^2$ any more. Of course, as long as the dip is apparent the presence of the interference is notable, and it would not be difficult to analyze the signal by taking into account this contribution. On the other hand, if the sign of $\delta n_1^0 + \delta n_2^0$ is the same as δn_{th}^0 , the contribution of the phase species grating is not obvious. In this case, if the deviation from the single exponential function is small, the apparent decay rate constant by a single exponential fitting is slower than $2D_{th}q^2$. The decay rate is easily misinterpreted. Even a minor contribution of the species grating changes the apparent decay rate dramatically.

When the LO light is introduced, the signal is enhanced as stated in the previous section (Figure 3(b)). At the same time, signal is linearized so that now the decay of the thermal grating component is clearly seen without the interference between two components and the decay rate constant ($D_{th}q^2$) can be determined directly. The OHD-TG signals at various $\Delta\phi$ are shown in Figure 3(c). The phase angle $\Delta\phi$ was set by slightly tilting

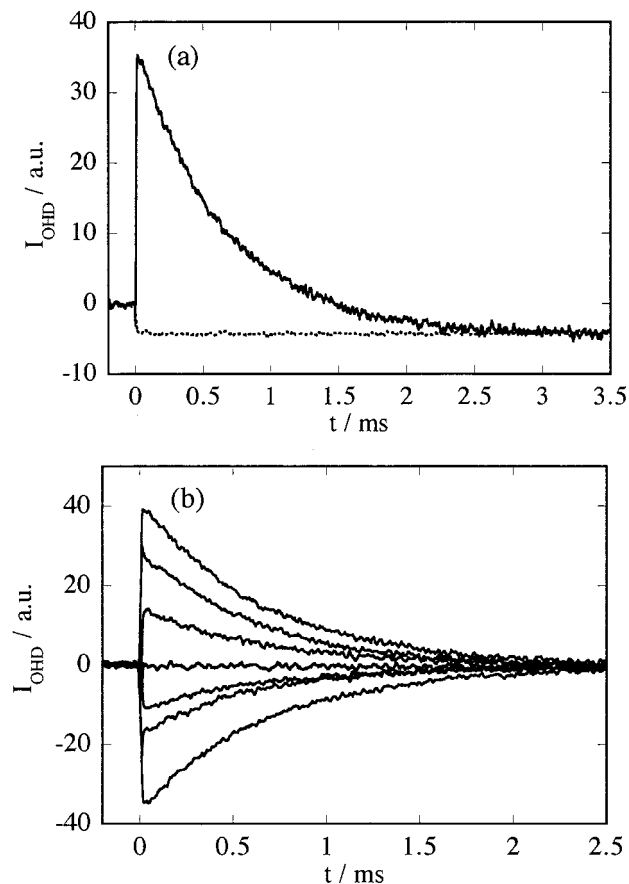


Figure 4. (a) The OHD species grating signal in a longer time scale. Since the TL signal contributes to the signal, the baseline in the $t > 3 \mu s$ region is lower than the intensity at $t < 0$. The dotted line is the signal without the probe light. (b) The OHD signal at various angles after the correction of the TL and transient absorption contributions.

the ND filter. The relative phase difference was determined from the intensity of the thermal grating signal. As described in the previous section, the phase difference at the maximum thermal grating intensity should be $\Delta\phi = 0^\circ$. The angle where the thermal grating signal disappears is $\Delta\phi = 90^\circ$ and 270° . The intermediate angle was determined by the signal fitting with eq 5. (The thermal grating intensity should be the same at $\Delta\phi$ and $360^\circ - \Delta\phi$. Here, $\Delta\phi$ and $360^\circ - \Delta\phi$ are discriminated by the sign of the δk term ($\delta k > 0$ for $0 < \Delta\phi < 180^\circ$.) We believe that using the thermal grating signal as a reference signal for the determination of $\Delta\phi$ is the most appropriate way in the TG experiment under the photoexcitation condition because of the following reasons. First, whenever materials are photoexcited, heat release from the excited state is always expected by the nonradiative transition and the thermal grating signal appears. Hence, we can use this component for most of the experiments. Second, this component generally consists of the (nearly pure) phase grating and it is easy to calculate the phase difference without any complicated interpretations. Third, since the decay rate constant of the thermal grating signal is determined by the thermal diffusion ($D_{th}q^2$), this signal can be easily identified and the intensity can be accurately measured by the exponential fitting. Even in a faster time scale (such as in picosecond ranges), the thermal contribution appears as an acoustic signal and it is easy to identify the component from the characteristic oscillating feature.¹⁵

The observed signals can be consistently reproduced very well by a calculation of eqs 5 and 6 (dotted line in Figure 3(c)). Although the phase fluctuation during one recording time (a

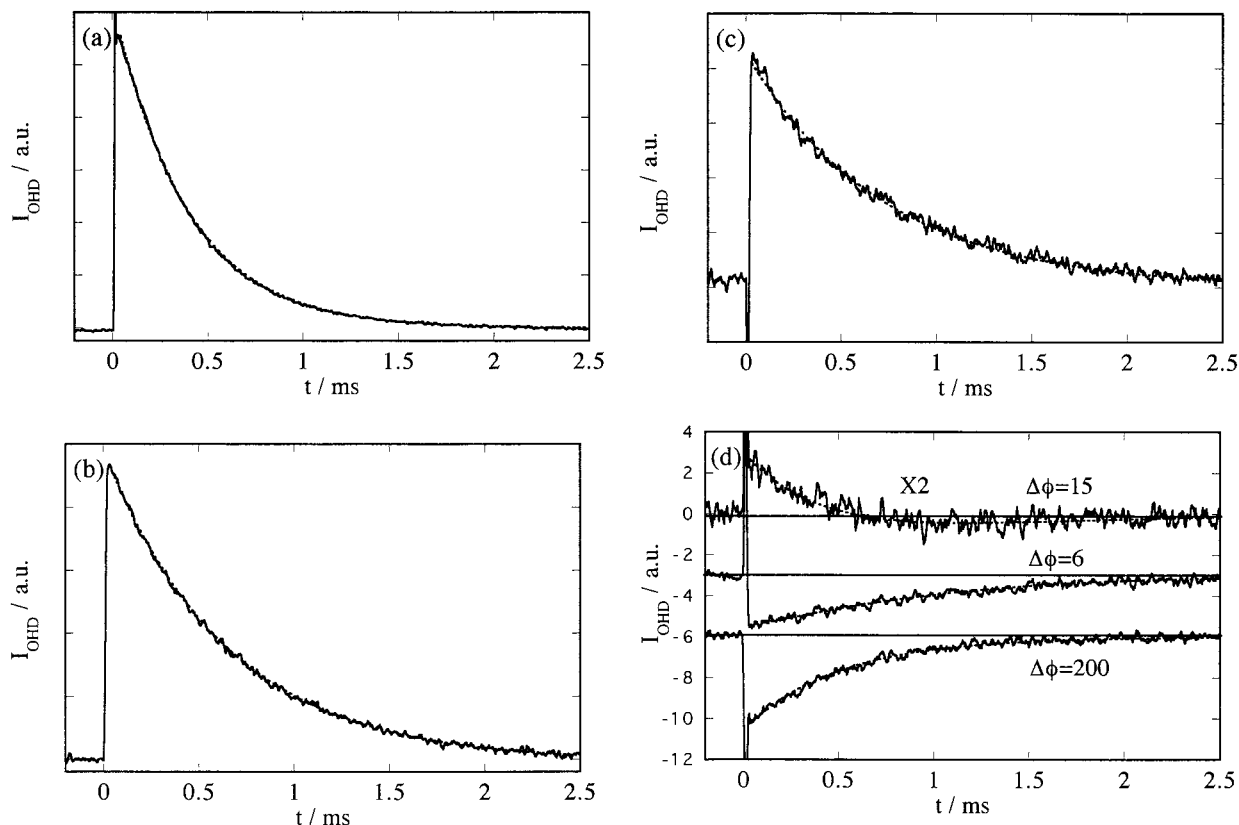


Figure 5. (a) Homodyne detected species grating signal of THS in ethanol. (b) The pure amplitude grating signal. (c) The pure phase grating signal. (d) The OHD-TG signal at angles to reduce the mercyanine contribution. The dotted lines are the best fitted curves by a single exponential function (a~c) and a biexponential function (d). The observed and calculated curves are almost perfectly overlapped in a~c within our S/N range. The numbers listed in the figure indicate the phase angles in degree between the probe and LO fields. They were determined by the signal fitting with eq 5. The error of the phase angle is $\pm 2^\circ$.

few ms) can be completely neglected, there may be a phase fluctuation during the averaging duration (~ 2 s). For that case, the determined phase angle should be considered as an average $\Delta\phi$ during the measurement. The uncertainty of the phase by the fitting is estimated as $\Delta\phi = \pm 2^\circ$.

Figure 4 shows the OHD-TG signals in a longer time scale. The decay of the species grating signal is clearly observed. The signal decays to a baseline that is slightly different from the position in the $t < 0$ region. A part of this shift is the effect of the thermal lens as shown previously.¹⁹ However, for this spiropyran molecule probed at 633 nm wavelength, an additional component, transient absorption by the mercyanine form, should contribute to the baseline shift. The contribution of the thermal lens effect in the phase grating signal can be eliminated by subtracting the baseline measured with blocking the probe beam or by subtracting the $\Delta\phi = 180^\circ$ signal from the $\Delta\phi = 0^\circ$ signal. The weakening of the LO light by the transient absorption and thermal lens effect should be taken into account for a correct analysis. However, in this case, since the contribution of the transient absorption is very small (less than 2% of the LO intensity) and the contribution is almost constant in this time range, the baseline is just subtracted for the correction. After this correction, the OHD-TG signals in a longer time scale at various $\Delta\phi$ are shown in Figure 4(b).

3.3. Separation of the Phase and Amplitude Gratings and Different Chemical Species. Figure 5(a) shows the homodyne detected species grating signal of THS in a longer time scale. The initial spike-like signal is the thermal grating, and the interference dip between the thermal grating and the species grating is noticeable. Since there are two sources of the signal, the homodyne detected signal after the decay of the thermal

grating should be analyzed by

$$I_{TG}(t) = \alpha(\delta n_{sp}(t))^2 + \beta(\delta k_{sp}(t))^2 \quad (7)$$

$$= \alpha(\delta n_1^0 \exp(-D_s q^2 t) + \delta n_2^0 \exp(-D_m q^2 t))^2 + \beta(\delta k_2^0 \exp(-D_m q^2 t))^2$$

For a correct analysis, these exponential components should be separated. However, the separation is practically impossible from this decay curve even by the least-squares fitting. In fact, the profile can be expressed well even by a single exponential function with a lifetime of $390 \mu\text{s}$ (at $q^2 = 3.4 \times 10^{12} \text{ m}^{-2}$). The deviation from the single exponential fitting is very small.

First, we separate the amplitude (Figure 5(b)) and phase (Figure 5(c)) contributions by adjusting the phase. Again, the phase angle was set so that the thermal grating intensity becomes maximum ($\Delta\phi = 0^\circ$) or zero ($\Delta\phi = 90^\circ$), respectively. The amplitude grating should consist of only the mercyanine contribution, and the profile ($I_{OHD-k}(t)$) should be expressed by a single-exponential function

$$I_{OHD-k}(t) \propto \delta k_2^0 \exp(-D_m q^2 t) \quad (8)$$

The lifetime of the signal at $q^2 = 3.4 \times 10^{12} \text{ m}^{-2}$ is $645 \mu\text{s}$, which gives $D_m = 4.6 \times 10^{-10} \text{ m}^2 \text{ s}^{-1}$.

On the contrary, the phase grating signal should contain both the mercyanine and spiro form contributions. The different sign between the thermal grating and the species grating signals (Figure 5(c)) indicates that the sign of the dominant part of the species grating is positive as already stated in the previous

section. This positive sign means that the dominant contribution to the phase grating is again the merocyanine form. This is expected because the absorption band of the merocyanine form is much closer to the probe wavelength (633 nm) than that of the spiro form. The signal ($I_{\text{OHD}-n}$) should be analyzed by

$$I_{\text{OHD}-n}(t) \propto \{\delta n_1^0 \exp(-D_s q^2 t) + \delta n_2^0 \exp(-D_m q^2 t)\} \quad (9)$$

However, since the contribution of the spiro form is small even in this phase grating signal, the signal can be fitted rather well even by a single exponential function with a lifetime of 720 μs . The slightly longer lifetime of the phase grating compared with that of the amplitude grating (645 μs) results from a destructive overlapping of the spiro form signal in a faster time region of this signal.

Although we can successfully separate the phase and amplitude gratings, we cannot determine D_s from the phase grating signal, because the contribution of the merocyanine form is so dominant. As an interesting application of the OHD-TG method, we here demonstrate that the contributions from two chemical species can be separated. If we rewrite $I_{\text{OHD}}(t)$ as

$$I_{\text{OHD}}(t) \propto \delta n_{\text{th}}^0 \cos \Delta\phi \exp(-D_{\text{th}} q^2 t) + \delta n_1^0 \cos \Delta\phi \exp(D_s q^2 t) + (\delta n_2^0 \cos \Delta\phi + \delta k_2^0 \sin \Delta\phi) \exp(-D_m q^2 t) \quad (10)$$

we will notice that the merocyanine contribution can be reduced under a condition of $\delta n_2^0 \cos \Delta\phi \sim -\delta k_2^0 \sin \Delta\phi$. Considering $\delta n_2^0 > 0$, $\delta k_2^0 > 0$, and $\delta n_2^0 < \delta k_2^0$, we should find such a phase angle in a range of $0^\circ < \Delta\phi < 45^\circ$, or $180^\circ < \Delta\phi < 225^\circ$.

The OHD species grating signals measured at several $\Delta\phi$ in these regions are shown in Figure 5(d). (The tilt angle of the ND filter was roughly adjusted with monitoring the thermal grating signal. The accurate value of $\Delta\phi$ was determined later by the signal fitting with eq 5 as described in section 3-2.) Since the dominant part of the signal is eliminated, the signal intensity is weak. However, it is apparent that the decay of the signal is no more single exponential. It is also noted that the signal at an early time deviates from the exponential curve in the direction of the thermal grating, which is a consequence of the negative sign of δn_{th}^0 and δn_1^0 . This OHD-TG signal was fitted by the nonlinear least-squares method with a biexponential function. The lifetime of the longer component was fixed to the lifetime from the amplitude grating signal ($(D_m q^2)^{-1}$). The fitting was generally very good and the lifetime of the shorter component was $520 \pm 30 \mu\text{s}$. Considering the sign of this component ($\delta n_1^0 < 0$), we should assign this component to the spiro form contribution. From these lifetimes, we can determine the diffusion constants of both species as $D_s = 5.7 \times 10^{-10} \text{ m}^2 \text{ s}^{-1}$ and $D_m = 4.6 \times 10^{-10} \text{ m}^2 \text{ s}^{-1}$.

Frequently, the diffusion constant in solution is calculated using the Stokes–Einstein relationship

$$D_{\text{SE}} = kT/a\eta$$

where a is a constant ($a = 4\pi$ for the slip boundary condition and $a = 6\pi$ for the stick boundary), r is a radius, and η is the viscosity. If we estimate r by an atom increment method,²⁴ D_{SE} of THS for the slip and stick boundary conditions are calculated to be $7.5 \times 10^{-10} \text{ m}^2 \text{ s}^{-1}$ and $5.0 \times 10^{-10} \text{ m}^2 \text{ s}^{-1}$, respectively. Here, D_m is relatively close to D_{SE} under the stick boundary condition. The smaller D_m compared with D_s can be interpreted

in terms of the effect of the charge separation of the merocyanine form. The large dipole moment increases the translational friction between the solute and solvent compared with relatively nonpolar form of the spiro-THS.

In a previous paper, we had difficulty determining D_s and D_m of a similar spiroopyran (1',3',3'-trimethyl-8-nitrospiro(2H-1-benzopyran-2,2'-indoline)), because the merocyanine form possesses a strong absorption at 633 nm which gives rise to a predominant TG signal over the spiro form. At that time, we used a different probe wavelength that was located between the spiro and merocyanine absorption bands. Even using this wavelength, however, the merocyanine contribution dominated the spiro contribution and biexponential fitting was difficult. The selective reduction of one species by the OHD-TG technique will be a great advantage for studying photochemical reactions.

Summary

The TG signal is frequently complicated by various contributions, such as the phase and amplitude gratings and by contributions from several chemical species. The entanglement should be separated for a correct interpretation of the signal. In this report, by adjusting the phase between the probe and LO fields, we actually separated not only the phase and amplitude contributions but also the signals from two chemical species: the merocyanine and spiro forms of a spiroopyran molecule. Using the phase adjustment, the signal from the merocyanine form can be suppressed and the diffusion constant of the spiro form can be determined even under a condition that the dominant part of the homodyne detected signal comes from the merocyanine form.

Acknowledgment. The author is indebted to Prof. N. Hirota for his discussions and encouragement. A part of this study was supported by the Grant-in-Aid on Priority Area of Chemical Reaction Dynamics in Condensed Phase (10206202).

References and Notes

- (1) Eichler, H. J.; Günter, P.; Pohl, D. W. *Laser induced dynamic gratings*, Springer-Verlag: Berlin, 1986.
- (2) Fayer, M.D. *Annu. Rev. Phys. Chem.* **1982**, *33*, 63.
- (3) Dhar, L.; Rogers, J. A.; Nelson, K. A. *Chem. Rev.* **1994**, *94*, 157.
- (4) Miller, R. J. D. In *Time resolved spectroscopy*; Clark, R. J. H., Hester, R. E., Eds.; John Wiley & Sons, 1989.
- (5) Kogelnik, H. *Bell. System Technol. J.* **1969**, *48*, 2909.
- (6) Shen, Y. R. *The principle of nonlinear optics*; John Wiley & Sons: New York, 1984.
- (7) Terazima, M. *Res. Chem. Intermed.* **1997**, *23*, 853.
- (8) Terazima, M. *Adv. Photochem.* **1998**, *24*, 255.
- (9) Vöhringer, P.; Scherer, N. F. *J. Phys. Chem.* **1995**, *99*, 2684.
- (10) Köhler, W. Rossmanith, P. *J. Phys. Chem.* **1995**, *99*, 5838.
- (11) Matsuo, S.; Tahara, T. *Chem. Phys. Lett.* **1997**, *264*, 636.
- (12) Chang, Y. J.; Cong, P.; Simon, J. D. *J. Phys. Chem.* **1995**, *99*, 7857.
- (13) Rogers, J. A.; Fuchs, M.; Banet, M. J.; Hanselman, J. B.; Logan, R.; Nelson, K. A. *Appl. Phys. Lett.* **1997**, *71*, 225.
- (14) Maznev, A. A.; Nelson, K. A.; Rogers, J. A. *Opt. Lett.* **1998**, *23*, 1319. Maznev, A. A.; Crimmins, T. F.; Nelson, K. A. *Opt. Lett.* **1998**, *23*, 1378.
- (15) Goodno, G. D.; Dadusc, G.; Miller, R. J. D. *J. Opt. Soc. Am. B* **1998**, *15*, 1791. Dadusc, G.; Goodno, G. D.; Chiu, H.-L.; Ogilvie, J.; Miller, R. J. D. *Israel J. Chem.* **1998**, *38*, 191.
- (16) Strauss, J.; Hundhausen, M.; Ley, L. *Appl. Phys. Lett.* **1996**, *69*, 875.
- (17) Goodno, G. D.; Astinov, V.; Miller, R. J. D., submitted.
- (18) Högemann, C.; Vauthey, E. *Israel J. Chem.* **1998**, *38*, 181.
- (19) Terazima, M. *Chem. Phys. Lett.* **1999**, *304*, 343.

(20) Gallagher, S. M.; Albrecht, A. W.; Hybl, J. D.; Landin, B. L.; Rajaram, B.; Jonas, D. M. *J. Opt. Soc. Am. B* **1998**, 8, 2338.

(21) *Photochromism, Techniques of Chemistry*, Brown, G. H., Ed.; Wiley: New York, 1971. Herve, H.; Leger, L.; Rondelez, F. *Phys. Rev. Lett.* **1979**, 42, 1681.

(22) Okazaki, T.; Hirota, N.; Terazima, M. *J. Photochem. Photobiol.* **1996**, 99, 155.

(23) Takezaki, M.; Hirota, N.; Terazima, M. *J. Phys. Chem. A* **1997**, 101, 3443.

(24) Bondi, A. *J. Phys. Chem.* **1964**, 68, 441.